

Delayed Magnetic Catalysis

Jens Braun,^{1,2} Walid Ahmed Mian,¹ and Stefan Rechenberger¹

¹*Institut für Kernphysik (Theoriezentrum), Technische Universität Darmstadt, D-64289 Darmstadt, Germany*

²*ExtreMe Matter Institute EMMI, GSI, Planckstraße 1, D-64291 Darmstadt, Germany*

We study the effect of an external magnetic field on the chiral phase transition in the theory of the strong interaction by means of a renormalization-group (RG) fixed-point analysis, relying on only one physical input parameter, the strong coupling at a given large momentum scale. To be specific, we consider the interplay of the RG flow of four-quark interactions and the running gauge coupling. Depending on the temperature and the strength of the magnetic field, the gauge coupling can drive the quark sector to criticality, resulting in chiral symmetry breaking. In accordance with lattice Monte-Carlo simulations, we find that the chiral phase transition temperature decreases for small values of the external magnetic field. For large magnetic field strengths, however, our fixed-point study predicts that the phase transition temperature increases monotonically.

Introduction.— The dynamics of gauge theories is expected to be strongly affected by external magnetic fields. This is of great phenomenological relevance for a large variety of systems, ranging from condensed-matter theory [1, 2] over off-central heavy-ion collision experiments [3, 4] to neutron stars [5] and cosmological models [6]. In fact, studies of the influence of an external magnetic field on the phase diagram of the theory of the strong interaction (Quantum Chromodynamics, QCD) and its equation of state have attracted a lot of attention in recent years. In particular, the peculiar inverse-catalysis effect is here of great interest [7]. It is related to the observation that the chiral critical temperature decreases with increasing strength of the magnetic field, in contradistinction to purely fermionic models also known from condensed-matter theory where magnetic catalysis is observed, i.e. the critical temperature increases with increasing magnetic field strength [1, 8].

The observation of inverse catalysis in lattice Monte-Carlo (MC) studies of the chiral phase transition in QCD has come unexpected [7]. This is related to the fact that effective low-energy QCD models are commonly believed to describe correctly many features of the QCD phase diagram, at least on a qualitative level. Since these models are predominantly purely fermionic models being close relatives to the Nambu–Jona-Lasinio model, which has been originally constructed based on analogies to condensed-matter theory [9], it also appeared natural to expect that only magnetic catalysis is at work in QCD [10, 11], see Ref. [12] for reviews.

Various extensions of low-energy QCD models have been studied, ranging from the inclusion of the order-parameter for deconfinement as obtained from lattice MC simulations [13] to extensions beyond the mean-field approximation [14, 15]. Moreover, the effect of a magnetic field on the chiral dynamics has been recently studied using Dyson-Schwinger equations (DSE) [16]. In any case, the very observation of magnetic catalysis is found to be generic, even if effects associated with the chiral anomaly are taken into account [10]. On the other hand, it has been found that the parameters of low-energy models can

be tuned such that inverse catalysis occurs at weak magnetic fields [17, 18]. Interestingly, at strong magnetic fields, catalysis is still observed and appears to be a robust feature of these models.

The detailed analysis of low-energy models suggests that a formulation of the problem in terms of microscopic degrees of freedom has the greatest potential to explain the appearance of the inverse-catalysis effect. In particular, the dependence of the running coupling on the magnetic field is expected to play a prominent role in a dynamical study of chiral symmetry breaking [19, 20].

In this work, we analyze the origin of the inverse-catalysis effect in finite-temperature QCD. To this end, we discuss the chiral quark dynamics in the presence of an external magnetic field by studying the underlying fixed-point structure. In particular, we shall point out that the dependence of the chiral dynamics on the external magnetic field is governed by an intriguing interplay between the quark and gluon degrees of freedom. However, we also emphasize that we are not aiming at quantitative precision with our analysis but rather aim at revealing the mechanisms and the connection underlying inverse catalysis observed in lattice MC simulations and magnetic catalysis being a well-established phenomenon in the context of condensed-matter systems.

Formalism.— The starting point for our analysis is the classical action S in $4d$ Euclidean space-time,

$$S = \int d^4x \left\{ \frac{1}{4} F_{\mu\nu} F_{\mu\nu} + \bar{\psi} (i\not{D} + \bar{g}\not{A} + \bar{e}\not{\mathcal{A}}) \psi \right\}, \quad (1)$$

where \bar{g} is the bare gauge coupling and $\bar{e} \equiv e$ denotes the electric charge. The non-Abelian fields A_μ enter the definition of the field-strength tensor $F_{\mu\nu}$ and are associated with the gluon degrees of freedom. The external electrodynamic potential is determined by $\mathcal{A}_\mu = (0, 0, Bx_1, 0)$, where the magnetic field B is assumed to be spatially and temporarily constant. In the present work we shall moreover restrict ourselves to the case of two massless quark flavors.

The quark-gluon interaction in Eq. (1) induces quark self-interactions, e. g. by two-gluon exchange. Chiral

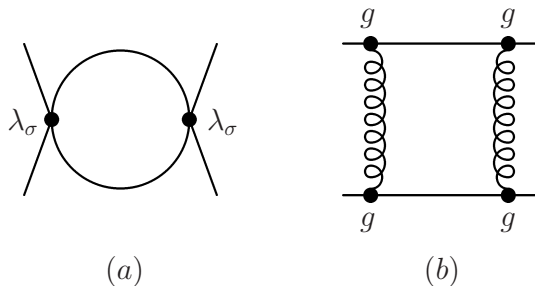


Figure 1. The depicted Feynman diagrams labelled with (a) and (b) are associated with the first and the third term on the right-hand side of Eq. (2), respectively. The second term associated with the so-called triangle diagram is not shown, as it plays only a subleading role in our analysis.

symmetry breaking is then ultimately triggered by the four-quark interactions approaching criticality, i.e. the associated couplings become relevant. In our study we shall only consider one particular four-quark interaction channel, namely the scalar-pseudoscalar channel. This channel can be used to monitor spontaneous chiral symmetry breaking and has been found to be the most dominant one in Fierz-complete studies, both at zero [21, 22] and finite temperature [23]. At finite external magnetic field, the number of interaction channels in a Fierz-complete basis increases considerably due to the strong explicit breaking of Poincaré invariance [24, 25]. For our more qualitative analysis of the mechanisms underlying chiral symmetry breaking, however, we shall drop these additional channels for simplicity.

The renormalization-group (RG) β -function of the four-quark coupling λ_σ associated with the scalar-pseudoscalar interaction channel is given by

$$\partial_t \lambda_\sigma = 2\lambda_\sigma^2 - l_{\lambda_\sigma^2} \lambda_\sigma^2 - l_{\lambda_\sigma g^2} \lambda_\sigma g^2 - l_{g^4} g^4, \quad (2)$$

where $t = \ln(k/\Lambda)$ is the so-called RG ‘time’ with k being the RG scale and Λ being an ultraviolet (UV) cutoff scale at which we fix the initial conditions, e.g. the τ -mass scale. The couplings $\lambda_\sigma \sim k^2 \bar{\lambda}_\sigma$ and g are dimensionless and assumed to be suitably renormalized. The first term on the right-hand side describes simply the dimensional scaling of the coupling. The quantities $l_{\lambda_\sigma^2} > 0$, $l_{\lambda_\sigma g^2} > 0$, and $l_{g^4} > 0$ are related to one-particle irreducible (1PI) Feynman diagrams, see Fig. 1, and depend on the dimensionless magnetic field $b = eB/k^2$, the dimensionless temperature $\tau = T/k$ and combinatoric factors. With respect to our numerical studies below, we add that Eq. (2) can also be derived from nonperturbative flow equations in the limit of point-like interactions. Here, we employ an RG equation for the quantum effective action [26]. Our RG flow then takes into account resummations of all diagram types shown in Fig. 1, including ladder diagrams. The details of the Wilsonian momentum-shell integrations are specified by the choice for a so-called regulator function in this case. Here, we shall use the exponential

regulator [26, 27].

The initial condition for the four-quark coupling is fixed by the classical action (1) and is therefore given by $\lambda_\sigma = 0$ at $k = \Lambda \gg \Lambda_{\text{QCD}}$ in the perturbative high-momentum regime. Thus, the quark self-interactions in our study are originally gluon-induced due to the term $\sim g^4$ in Eq. (2) and the associated coupling λ_σ does not represent a (free) parameter. The *only* parameter used in our numerical study below is the value of the strong coupling $g^2/(4\pi) \approx 0.322$ at the τ -mass scale $m_\tau \approx 1.78$ GeV which determines the physical scale [28].

Fixed-point analysis. – As indicated above, chiral symmetry breaking is triggered by the four-quark interaction approaching criticality, i.e. the associated coupling λ_σ diverges in the RG flow at a finite scale. In fact, since the four-quark coupling λ_σ is the inverse mass parameter of a Ginzburg-Landau effective potential for the chiral order parameter, such a divergence indicates the onset of chiral symmetry breaking, see Ref. [29] for a review.

Let us now discuss spontaneous chiral symmetry breaking in QCD by analyzing the fixed-point structure of the flow equation (2). We begin with the limit $T = 0$ and $B = 0$, where the quantities $l_{\lambda_\sigma^2}$, $l_{\lambda_\sigma g^2}$, and l_{g^4} are simply numbers. At weak gauge coupling, quark self-interactions are exclusively generated by gluon exchange processes. For increasing gauge coupling, the two fixed points of the four-quark coupling then approach each other, see Fig. 2. Provided that the gauge coupling does not exceed a critical value, $g^2 \leq g_{\text{cr}}^2$, the four-quark coupling approaches a fixed point in the infrared and therefore remains finite. Thus, the system stays in the chirally symmetric phase. However, if the gauge coupling exceeds the critical value g_{cr}^2 at some scale, then the four-quark coupling λ_σ is no longer bounded by fixed points. In fact, λ_σ grows rapidly and approaches a divergence at a finite scale, indicating chiral symmetry breaking.

At $T > 0$ and $B = 0$, the loop integrals parametrized by the quantities $l_{\lambda_\sigma^2}$, $l_{\lambda_\sigma g^2}$, and l_{g^4} become functions of the dimensionless temperature $\tau = T/k$. For large scales $k \gg T$, these functions approach their zero-temperature values and the dynamics of the matter sector as measured by the fixed points remains unchanged. For high temperatures (or small scales) $T \gg k$, on the other hand, the quarks acquire a large thermal mass and thus stronger interactions are required to drive the quarks to criticality. In other words, the critical value for the gauge coupling g_{cr}^2 increases monotonically for increasing T/k . In fact, we have $l_{\lambda_\sigma^2} \rightarrow 0$, $l_{\lambda_\sigma g^2} \rightarrow 0$, and $l_{g^4} \rightarrow 0$ for $T/k \rightarrow \infty$. This suggests chiral symmetry restoration at high temperatures. This simple picture of chiral symmetry breaking at zero and finite temperature has been put forward in Refs. [21, 23], and underlies subsequent studies of the infrared properties of QCD [22, 30].

We now discuss the fixed-point dynamics in the presence of an external magnetic field. To this end, we first note that the gluons do not carry an electric charge and

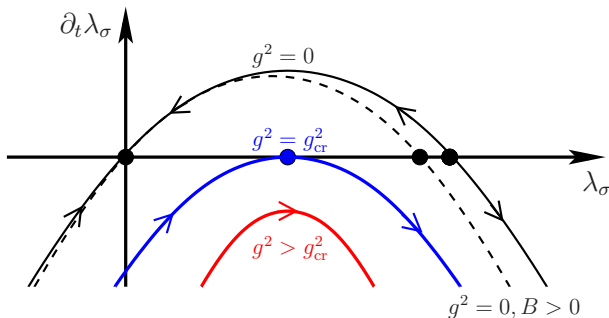


Figure 2. Sketch of the β function of the four-quark interaction λ_σ at $T = 0 = B$ (solid lines) as well as for $g^2 = 0$ and $B > 0$ (dashed line). The arrows indicate the direction of the flow towards the infrared.

are therefore not directly affected by the presence of an external magnetic field. On the other hand, the quarks are electrically charged and their dynamics is indeed altered. More specifically, the magnetic field can be associated with a length scale $\ell_B \sim (eB)^{-1/2}$. In the presence of this scale, the quark fields experience Landau-level quantization which comes along with a magnetic zero-mode (lowest Landau level) for the quark fields. This zero mode essentially governs the dynamics of the quarks, in particular in the large- b limit, where $b = eB/k^2$. In this work, we have computed the B -field dependence of the appearing loop integrals in the lowest Landau-level (LLL) approximation and suitably amended them to approach the correct result in the limit of large scales k , i.e. $b \rightarrow 0$. This ensures that the dynamics of the theory in the UV limit remains unchanged.

Let us begin our discussion of magnetic field effects with the zero-temperature limit. Moreover, it is instructive to consider first the case of vanishing gauge coupling. In this case, for increasing dimensionless magnetic field $b = eB/k^2$, the non-Gaussian fixed point is shifted to smaller values which entails that the maximum of the β function is also pushed to smaller values, see Fig. 2. This can be understood from the fact that the contribution from the quark loop increases monotonically with b . To be specific, we have $l_{\lambda_\sigma^2} \sim b$ in the large- b limit which is well-known from RG studies of fermionic models [14, 24]. In any case, the shift of the interacting fixed point towards the Gaussian fixed point for finite b and $g^2 = 0$ already suggests that g_{crit}^2 decreases with increasing b , at least in the large- b limit. This is indeed the case since we find that the box diagram scales as $l_{g^4} \sim b^{-1/2}$, resulting in $g_{\text{cr}}^2 \sim b^{-1/4}$ for large b , i.e. in the deep infrared limit. The triangle diagram $l_{\lambda_\sigma g^2} \sim 1$ plays only a sub-leading role in our analysis. Note that the b -dependence of the quark loop in the LLL approximation is identical to the b -scaling behavior of this diagram in the limit of asymptotically large magnetic fields. This is not the case for the triangle and the box diagram. Even in the LLL

approximation, the dependence of these diagrams on the magnetic field is more involved due to the internal gluon lines. The latter subtlety together with the observation that the term $\sim g^4$ in Eq. (2) is suppressed for finite b is of great importance: Lowering the scale k starting from a point in the UV regime with $g_{\text{cr}}^2(b) \approx g_{\text{cr}}^2(0)$, we find that the magnetic suppression of the box diagram yields an increase of g_{cr}^2 before it reaches a maximum and then approaches zero due to the magnetic enhancement of the quark loop in the infrared limit.

The scale dependence of g_{cr}^2 for a given finite temperature T and magnetic field B can now be understood from our discussion above. For large scales $k \gg T$ and $k \gg B$, the chiral critical coupling g_{cr}^2 approaches a finite constant value, $g_{\text{cr}}^2(b, \tau) \rightarrow g_{\text{cr}}^2(0, 0)$. Starting in the UV limit and lowering the scale k , we find that g_{cr}^2 increases. Most importantly, g_{cr}^2 becomes even larger than in the case $B=0$ for the same temperature due to the magnetic suppression of the box diagram. It is this increase of g_{cr}^2 on intermediate scales at finite B which favors inverse catalysis over catalysis for weak magnetic fields.

Running gauge coupling.— Our fixed-point analysis allows us to trace the question of the onset of chiral symmetry breaking back to the strength of the coupling g^2 relative to the critical coupling g_{cr}^2 . Therefore an actual determination of the QCD ground-state properties with respect to chiral symmetry requires information about the RG running of the strong coupling. To this end, we employ the results for the gauge coupling at zero and finite temperature from Refs. [23, 31] and restrict ourselves to Feynman gauge for simplicity. At zero temperature, the running of g^2 agrees well with perturbation theory for small coupling. In the infrared limit, on the other hand, the gauge coupling assumes a finite value associated with an a non-Gaussian fixed point. At finite temperature, the behavior of the coupling at large scales $k \gg T$ remains unaffected and still agrees well with the perturbative running in the zero-temperature limit. In the infrared limit, however, the running of the coupling has been found to be qualitatively distinct from the zero-temperature case [23]. In fact, the coupling decreases linearly with the scale k according to $g^2 \sim k/T$ and eventually tends to zero. In this regime, the flow of the running coupling is solely driven by the gluonic thermal zero-mode associated with the spatial $3d$ Yang-Mills theory. Thus, the infrared behavior of the coupling in $4d$ is directly related to the infrared behavior of the coupling in the underlying $3d$ theory: $g^2(k \ll T) \sim g_{3d,*}^2 k/T$ with $g_{3d,*}^2 \sim \mathcal{O}(1)$, see Ref. [23]. Moreover, we note that the running coupling is bounded from above on all scales and the maximum value of the coupling decreases with increasing temperature.

At finite magnetic field, the gauge coupling g^2 also depends on $b = eB/k^2$ due to the quark-gluon coupling. To better understand the effect of the magnetic field on g^2 , we consider the associated β function: $\partial_t g^2 = \eta_{g^2} g^2 = (\eta_A + \eta_q) g^2$, which we have conveniently

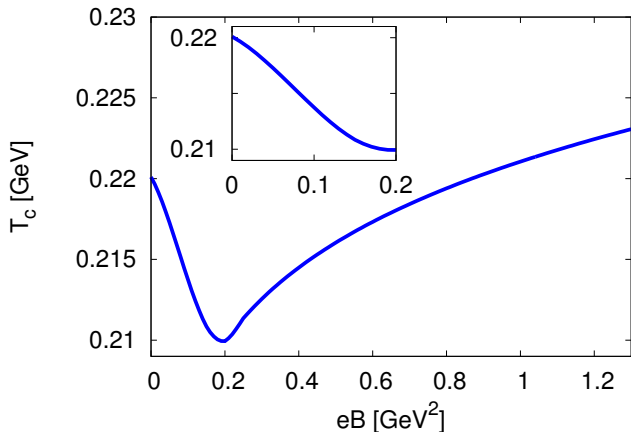


Figure 3. Chiral critical temperature T_c as a function of eB .

split into a purely gluonic contribution η_A and a contribution η_q containing all contributions from diagrams with internal quark lines. For example, at the one-loop level, $\eta_q \sim g^2$ is structurally identical to the vacuum polarisation tensor in Quantum Electrodynamics (QED). In the limit of large (dimensionless) magnetic fields, η_q is primarily determined by the dynamics of the magnetic zero mode of the quarks, resulting in $\eta_q \sim b$ at zero temperature as in QED [32]. Thus, the quark contribution η_q to the running coupling is magnetically enhanced compared to the gluon contribution η_A . This results in a decrease of the coupling in the infrared limit, $g^2 \rightarrow 0$ for $k \rightarrow 0$. Loosely speaking, the magnetic field acts as an increase of quark flavors towards the infrared limit, such that the gauge coupling is attracted by the Gaussian fixed point. In contrast to the finite-temperature case at $B = 0$, the behavior of the gauge coupling in the infrared can now not be straightforwardly related to the dynamics of a dimensionally reduced gauge theory: Whereas the quark fields experience a dimensional reduction from four to two dimensions for strong magnetic fields, the gluon fields are not directly affected and therefore are not dimensionally reduced in the infrared limit.

In the presence of a magnetic field at finite temperature, the running of the gauge coupling in the (deep) infrared is still governed by the underlying 3d Yang-Mills theory since the quarks decouple eventually from the flow due to their thermal Matsubara masses. In any case, for our numerical computation of the chiral critical temperature T_c as a function of the magnetic field B , we employed the results for the running gauge coupling from Ref. [23] and used only the B -field dependent one-loop expression for η_q in the LLL approximation to suitably amend the quark contribution η_q to η_{g^2} in the large- b limit; details will be presented elsewhere [33].

Magnetic phase diagram. – Using our numerical results for the scale-dependence of the chiral critical coupling g_{cr}^2

and the running gauge coupling g^2 , we can now compute the dependence of the chiral phase transition temperature T_c on the magnetic field B . To be specific, we estimate T_c as the lowest temperature for which no intersection point between g^2 and g_{cr}^2 as a function of k occurs for a given value of the magnetic field B . In Fig. 3, we show T_c as a function of eB . For $B = 0$, we find $T_c \approx 220$ MeV. The difference to the accepted value for the critical temperature from lattice QCD simulations [34] can be traced back to the fact that we did not consider a Fierz-complete set of four-quark interactions [23]. In any case, increasing the magnetic field B , we find that the critical temperature T_c decreases as also observed in lattice MC simulations [7]. We note that this decrease of T_c persists, even if we consider a B -independent running coupling. Thus, this decrease in the phase transition temperature can be traced back to the dynamics in the matter sector as discussed above in terms of our fixed-point analysis. The effective decrease of the gauge coupling at finite magnetic field only intensifies the inverse-catalysis effect in our analysis.

Increasing the magnetic field further, we observe that $T_c(eB)$ assumes a minimum at $eB \approx 0.2 \text{ GeV}^2$ and then increases for larger values of eB . Indications for such an increase at strong magnetic fields are also seen in a DSE study [35]. The catalysis effect for large eB can be traced back to the fact that the RG running of the four-quark interaction is mainly driven by the quark loop at strong magnetic fields. This results in a decrease of the critical coupling g_{cr}^2 and, in turn, in an increase of the critical temperature. Thus, the well-established magnetic catalysis effect in fermionic theories, which is simply driven by the fermion loop in Fig. 1 (a), sets in “delayed” due to the non-trivial quark-gluon dynamics in the matter sector.

Conclusions. – We have computed the phase diagram of QCD in the plane of temperature and magnetic field. Our results confirm the existence of the inverse-catalysis effect. Compared to lattice MC results for 2 + 1 (massive) quark flavors [7], our RG analysis predicts a smaller regime in which inverse catalysis occurs. Clearly, our simple study based on a single four-quark channel cannot be expected to be quantitative. Still, it appears worthwhile to study the scaling of the size of the inverse-catalysis regime when the number of quark flavors is increased. In any case, for large magnetic fields, we observe magnetic catalysis. Our fixed-point analysis reveals a simple mechanism for inverse magnetic catalysis at weak magnetic fields and, at the same time, explains the dynamics underlying the observed magnetic catalysis at strong magnetic fields. In this respect, the observed “delayed” magnetic catalysis can be viewed as a testable prediction for future lattice MC studies. Moreover, our simple analysis represents a promising starting point for phenomenological applications, such as the microscopically guided improvement of well-established QCD models.

Acknowledgments.— The authors thank H. Gies, F. Karbstein, J. M. Pawlowski, D. Roscher, and D. D. Scherer for useful discussions. Moreover, the authors are grateful to H. Gies and J. M. Pawlowski for comments on the manuscript. J.B. and S.R. acknowledge support by HIC for FAIR within the LOEWE program of the State of Hesse as well as by the DFG under grant SFB 634.

-
- [1] V. Gusynin, V. Miransky, and I. Shovkovy, *Phys.Rev.* **D52**, 4718 (1995).
- [2] V. P. Gusynin and S. G. Sharapov, *Phys.Rev.Lett.* **95**, 146801 (2005).
- [3] D. E. Kharzeev, L. D. McLerran, and H. J. Warringa, *Nucl.Phys.* **A803**, 227 (2008).
- [4] V. Skokov, A. Y. Illarionov, and V. Toneev, *Int.J.Mod.Phys.* **A24**, 5925 (2009).
- [5] R. C. Duncan and C. Thompson, *Astrophys. J.* **392**, L9 (1992).
- [6] T. Vachaspati, *Phys. Lett.* **B265**, 258 (1991).
- [7] G. Bali, F. Bruckmann, G. Endrodi, Z. Fodor, S. Katz, et al., *JHEP* **1202**, 044 (2012); *Phys.Rev.* **D86**, 071502 (2012).
- [8] V. Gusynin, V. Miransky, and I. Shovkovy, *Phys.Lett.* **B349**, 477 (1995); *Nucl.Phys.* **B462**, 249 (1996).
- [9] Y. Nambu and G. Jona-Lasinio, *Phys. Rev.* **122**, 345 (1961); *Phys. Rev.* **124**, 246 (1961).
- [10] A. Osipov, B. Hiller, A. Blin, and J. da Providencia, *Phys.Lett.* **B650**, 262 (2007).
- [11] E. S. Fraga and A. J. Mizher, *Phys.Rev.* **D78**, 025016 (2008).
- [12] I. A. Shovkovy, *Lect.Notes Phys.* **871**, 13 (2013); J. O. Andersen, W. R. Naylor, and A. Tranberg, arXiv:1411.7176 [hep-ph].
- [13] A. J. Mizher, M. Chernodub, and E. S. Fraga, *Phys.Rev.* **D82**, 105016 (2010); R. Gatto and M. Ruggieri, *Phys.Rev.* **D82**, 054027 (2010); *Phys.Rev.* **D83**, 034016 (2011); K. Kashiwa, *Phys.Rev.* **D83**, 117901 (2011).
- [14] K. Fukushima and J. M. Pawlowski, *Phys.Rev.* **D86**, 076013 (2012).
- [15] V. Skokov, *Phys.Rev.* **D85**, 034026 (2012); K. Kamikado and T. Kanazawa, *JHEP* **1403**, 009 (2014); arXiv:1410.6253 [hep-ph].
- [16] N. Mueller, J. A. Bonnet, and C. S. Fischer, *Phys.Rev.* **D89**, 094023 (2014).
- [17] E. Fraga, B. Mintz, and J. Schaffner-Bielich, *Phys.Lett.* **B731**, 154 (2014).
- [18] M. Ferreira, P. Costa, O. Lourenço, T. Frederico, and C. Providência, *Phys.Rev.* **D89**, 116011 (2014).
- [19] R. Farias, K. Gomes, G. Krein, and M. Pinto, *Phys.Rev.* **C90**, 025203 (2014).
- [20] E. Ferrer, V. de la Incera, and X. Wen, (2014), arXiv:1407.3503 [nucl-th].
- [21] H. Gies and J. Jaeckel, *Eur.Phys.J.* **C46**, 433 (2006).
- [22] M. Mitter, J. M. Pawlowski, and N. Strodthoff, (2014), arXiv:1411.7978 [hep-ph].
- [23] J. Braun and H. Gies, *Phys.Lett.* **B645**, 53 (2007); *JHEP* **0606**, 024 (2006).
- [24] D. D. Scherer and H. Gies, *Phys.Rev.* **B85**, 195417 (2012).
- [25] E. J. Ferrer, V. de la Incera, I. Portillo, and M. Quiroz, *Phys.Rev.* **D89**, 085034 (2014).
- [26] C. Wetterich, *Phys.Lett.* **B301**, 90 (1993).
- [27] D. Jungnickel and C. Wetterich, *Phys.Rev.* **D53**, 5142 (1996).
- [28] S. Bethke, *Nucl.Phys.Proc.Suppl.* **135**, 345 (2004).
- [29] J. Braun, *J.Phys.* **G39**, 033001 (2012).
- [30] J. Braun, L. M. Haas, F. Marhauser, and J. M. Pawlowski, *Phys.Rev.Lett.* **106**, 022002 (2011); J. Braun, L. Fister, J. M. Pawlowski, and F. Rennecke, (2014), arXiv:1412.1045 [hep-ph].
- [31] H. Gies, *Phys.Rev.* **D66**, 025006 (2002).
- [32] F. Karbstein, L. Roessler, B. Dobrich, and H. Gies, *Int.J.Mod.Phys.Conf.Ser.* **14**, 403 (2012).
- [33] J. Braun, W. A. Mian, and S. Rechenberger, (in preparation).
- [34] Y. Aoki, G. Endrodi, Z. Fodor, S. Katz, and K. Szabo, *Nature* **443**, 675 (2006); Y. Aoki, Z. Fodor, S. Katz, and K. Szabo, *Phys.Lett.* **B643**, 46 (2006); M. Cheng, N. Christ, S. Datta, J. van der Heide, C. Jung, et al., *Phys.Rev.* **D77**, 014511 (2008).
- [35] N. Mueller and J. M. Pawlowski, (in preparation).